Research on Chemical Intermediates
https://doi.org/10.1007/s11164-019-04049-y

One-pot synthesis of 2-amino-3-cyanopyridines and hexahydroquinolines using eggshell-based nano-magnetic solid acid catalyst via anomeric-based oxidation

Tahere Akbarpoor[1] · **Ardeshir Khazaei**[1] · **Jaber Yousefi Seyf**[2] · **Negin Sarmasti**[1] · **Maryam Mahmoudiani Gilan**[1]

Received: 6 August 2019 / Accepted: 23 November 2019

Abstract

In the present research, the eggshell as a hazardous waste by European Union regulations was converted to a valuable catalyst, namely nano-$Fe_3O_4@(HSO_4)_2$. The as-prepared catalyst, first, was characterized using different techniques, including Fourier-transform infrared spectroscopy (FT-IR), X-ray diffraction (XRD), energy-dispersive X-ray spectroscopy (EDX), field emission scanning electron microscopy (FESEM), and transmission electron microscopy (TEM). Back-titration method confirmed the loading of a high surface density of acidic group, namely 8.8 mmol HSO_4 per gram of the catalyst. The catalytic property of the as-prepared catalyst was examined in the synthesis of 2-amino-3-cyanopyridines via anomeric-based oxidation (ABO), and hexahydroquinolines derivatives. High yield, short reaction time, solvent-free condition, waste to wealth, and optimization with the design of experiment are the major advantages of the present work. Taken together, these results suggest the conversion of waste to wealth products around the world and usage in organic transformation.

Electronic supplementary material The online version of this article (https://doi.org/10.1007/s11164-019-04049-y) contains supplementary material, which is available to authorized users.

✉ Ardeshir Khazaei
khazaei_1326@yahoo.com

[1] Faculty of Chemistry, Bu-Ali Sina University, Hamedan 6517838683, Iran

[2] Department of Chemical Engineering, Hamedan University of Technology, Hamedan, Iran

Graphic abstract

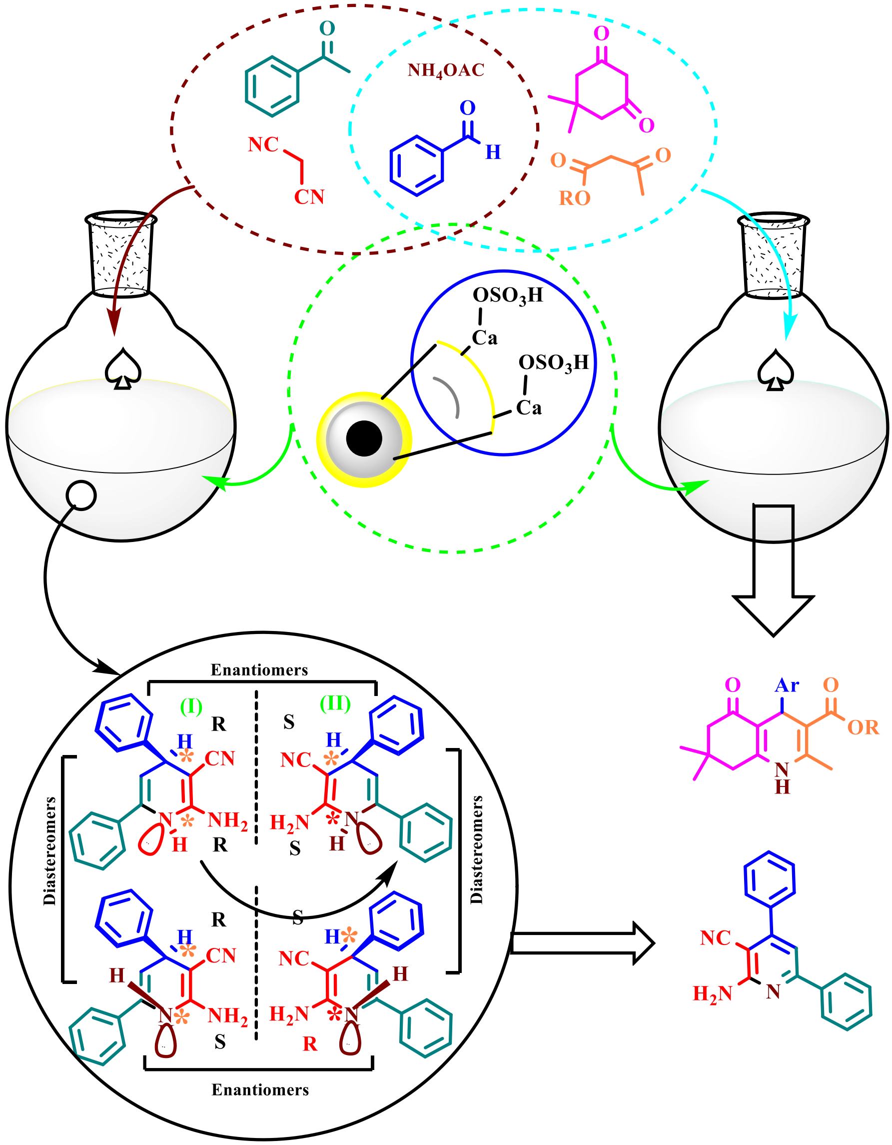

Keywords Eggshell · Nano-Fe_3O_4@$Ca(HSO_4)_2$ · Hexahydroquinoline · 2-amino-3-cyanopyridine

Introduction

Multicomponent reactions (MCRs) are chemical transformations which involve three or more reactants to react, providing diverse arrays of compounds. MCR is an important component in organic transformations and plays a key role in synthesis of heterocyclic moieties which in turn leads to chemical libraries containing a variety of biologically active components [1, 2]. On the other hand, MCRs are economically viable, high convergence with high bond-forming-index (BFI) [3] which has seen a resurgence of interest. Quinoline and its derivatives are a primary moiety in several natural products and medications, widely utilized in the pharmaceutical synthesis [4]. Quinolines with a 1,4-dihydropyridine (1,4-DHP) framework have numerous pharmaceutical properties [5]. Several methods have been proposed for the synthesis of quinolines, but each of them has shortcomings that include long reaction times, use of organic solvents, poor performance, harsh reaction conditions, expensive catalysts, etc. [6].

2-aminopyridines (2-APs) are key initial moieties in the synthesis of nitrogen heterocyclic compounds [7]. For instance, 2-aminopyridines are used in the synthesis of pharmaceuticals, such as piroxicam, sulfapyridine, tenoxicam, and tripelennamine [8]. Some decorated 2-AP is called 2-amino-3-cyanopyridines (2-A-3-CPs) which have interesting pharmacological properties [9]. The preparation of 2-A-3-CP can be traced back to the work of Kambe and Saito in the modified Chichibabin synthesis [10]. They synthesized 2-A-3-CP from separated arylidene malononitrile intermediate in a multicomponent reaction (MCR). Their methodology has disadvantages, including the use of benzene as a solvent, long reaction time, and low to moderate yield. 2-A-3-CPs have biological activities such as dual-target activities against VEGFR2 and Src [11], a potent inhibitor of HIV-1 integrase [12], antimicrobial agents [12], novel IKK-β inhibitors [13], A_{2A} adenosine receptor antagonists [14], and antiproliferative effect.

Although several methodologies have been reported for the synthesis of these molecules in the literature [15], these methods are limited to moderate yield, and long reaction time and use of volatile organic solvents (benzene [10], toluene [16], ethanol [13, 16–18], acetic acid [19], and 1,4-dioxane [20], 2,2,2-trifluoroethanol [21], dimethoxyethane [22]). On the other hand, 2-A-3-CP derivatives are synthesized using various catalyst, including the use of TBBDA and PBBS in solvent-free condition [9], $Ti(dpma)(NMe_2)_2$, $Ti(dpm)(NMe_2)_2$, and DMU [16, 23], copper nanoparticles [24], grindstone technology [25], ytterbium perfluorooctanoate [17], nano-Fe_3O_4 [18], $[Fe_3O_4\text{-}SiO_2\text{-}(CH_2)_3Im]C(CN)_3$ [26], cellulose sulfuric acid [27], $Pd(OH)_2$ [22], ClO_4^-/Al-MCM-41 [28], graphene oxide [29], urease [30], hexadecyldimethylbenzyl ammonium bromide (HDMBAB) [31], Cu(I) [32], and fructose/maltose [33]. But many of the methods are suffering from drawbacks such as longer reaction time, especially difficulty in catalyst preparation and separation. Our research group, recently, developed nano-Fe_3O_4@$(HSO_4)_2$ from the eggshell powder as a solid acid catalyst so that it was used in the synthesis of indazolo[1,2-b]-phthalazinetrione derivatives [34]. Accordingly, the aim of this research project has therefore been to investigate the efficacy of nano-Fe_3O_4@

$(HSO_4)_2$ in the synthesis of hexahydroquinolines and 2-amino-3-cyanopyridines derivatives. On the other hand, this research examines the significance of solvent-free condition, different solvents, temperature, and the amount of catalyst on the yield and the time of the chosen organic transformations.

Experimental section

General remarks

Ferrous chloride tetrahydrate ($FeCl_2{\cdot}4H_2O$), ferric chloride hexahydrate ($FeCl_3{\cdot}6H_2O$), ammonia (28 vol %), benzaldehyde, acetophenone, dimedone, ethanol, acetone, chloroform, and chlorosulfonic acid prepared from Merck Company. The reaction progress was monitored by TLC (EtOAc/*n*-hexane, 3/10) method. The ^{1}HNMR, ^{13}CNMR, and IR techniques together with a melting point were used to characterize the synthesized compounds. Spectral data provided in supporting information.

Preparation of Fe_3O_4 nanoparticles

The co-precipitation method [35] was used for preparation of the Fe_3O_4 magnetic nanoparticles. First, a solution was prepared by dissolving 11.3 g $FeCl_3{\cdot}6H_2O$ and 5.6 g $FeCl_2{\cdot}4H_2O$ in 100 mL deionized water at 80 °C. After the complete dissolution of the mentioned iron salts, 25 mL of ammonia was added to the mixture at once. A black dispersion of nano-Fe_3O_4 was obtained during 2 h at 80 °C under nitrogen atmosphere. Afterward, the resultant magnetic nanoparticles were collected using an external super magnet. The black magnetic nanoparticles were washed several times with water and acetone and finally dried in the oven.

Preparation of eggshell powder

Eggshells were immersed in boiling distilled water for 2 h and washed with it. The eggshells were dried in an oven at 120 °C for 2 h and milled using a cutting mill and then dried at 120 °C to obtain a constant weight. To remove any residue organic compounds, to a 100 mL dichloromethane in a 250-mL Erlenmeyer flask the eggshell powder was added and the mixture was homogenized in an ultrasound bath for 2 h. The eggshell powder was dried in an oven at 120 °C after separation through filtration.

Preparation of Fe_3O_4@eggshell

A mixture was prepared by adding 1 g of the prepared eggshell powder in the previous step to 100 mL water and stirred for 10 min. Then, 0.5 g of prepared nano-Fe_3O_4 was added to the mixture and dispersed using an ultrasound bath for 15 min and finally continuously stirred for 2 h at 60 °C. Eggshell powder ($CaCO_3$)

attaches to the nano-Fe_3O_4 surface via electrostatic (columbic) and electrodynamics forces [36]. These forces are strong enough to prevent separation of $CaCO_3$ from the nano-Fe_3O_4 core. Finally, the resultant nano-Fe_3O_4@eggshell was dried in an oven at 90 °C after filtration.

Preparation of $Fe_3O_4@Ca(HSO_4)_2$

To 100 mL of dried CH_2Cl_2, 1 g Fe_3O_4@eggshell was added and stirred for 15 min. Then, controlling the mixture temperature at 0 °C, 0.66 mL chlorosulfonic acid was gently added to the mixture. The temperature of the reaction should be hold at 0 °C to remove all gas from the reaction. The reaction mixture was stirred continuously for 24 h after exhausting all gases. The reaction between $CaCO_3$ and $ClSO_3H$ is as follows: $ClSO_3H + CaCO_3 \rightarrow CaCl_2 + Ca(HSO_4)_2 + HCl$ [34]. The obtained $Fe_3O_4@Ca(HSO_4)_2$ nanoparticles were separated from the mixture via a super magnet; then, it was dried in an oven after washing several times with water and CH_2Cl_2. Observation of gas generation during addition of chlorosulfonic acid confirms the production of HCl [34]. The procedure for the synthesis of nano-$Fe_3O_4@Ca(HSO_4)_2$ is shown in Fig. 1.

General synthesis of 2-amino-3-cyanopyridines derivatives

At solvent-free condition, 1 mmol benzaldehyde, 1 mmol acetophenone, 1.5 mmol ammonium acetate, and 1 mmol malononitrile (benchmark reaction 1) together with the 0.05 g as-prepared catalyst were added to a test tube at 90 °C (optimum reaction condition). Until the completion of reaction progress, it was monitored by a thin-layer chromatography (TLC) technique. The magnetic catalyst, then, was separated using a super magnet and dried in an oven after washing with water and ethanol. The final product was purified trough recrystallization in ethanol.

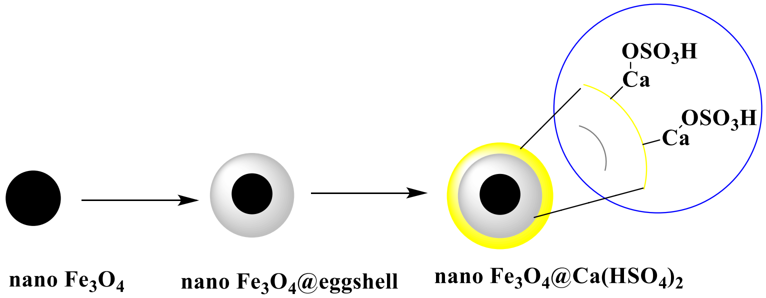

Fig. 1 Synthesis of nano-$Fe_3O_4@Ca(HSO_4)_2$

General procedure for the synthesis of hexahydroquinoline derivatives

At solvent-free condition, 1 mmol aldehyde, 1 mmol ethyl acetoacetate, 1 mmol dimedone, and 1.5 mmol ammonium acetate (benchmark reaction 2) together with 0.05 g catalyst were added to a test tube at 90 °C (optimum reaction condition). The progress of the reaction was checked via TLC, and after the completion of the reaction, the magnetic nanoparticles were separated using a super magnet, washed with water and ethanol, and dried in an oven. Finally, the pure product was obtained through recrystallization in ethyl acetate. All hexahydroquinoline derivatives were synthesized at the optimum reaction condition which was obtained for benchmark reaction 2.

Results and discussion

In the present research, first, the eggshell powder was coated on the surface of magnetic nano-Fe_3O_4, and then $CaCO_3$ as the main part of the eggshell was converted to $Ca(HSO_4)_2$ through reaction with $ClSO_3H$. Accordingly, a solid nano-magnetic acid catalyst (Fe_3O_4@$Ca(HSO_4)_2$) was synthesized and used in the organic transformations. That is, the eggshell turned into a solid, green, and environmentally friendly solid acid catalyst [34]. Based on the back-titration method, 5.18 mmol $–SO_4H$ group was loaded per gram of the prepared catalyst. Of more interest here was the evaluation of catalytic activity of the as-synthesized catalyst in the synthesis of 2-amino-3-cyanopyridine and hexahydroquinoline derivatives.

Characterization of the as-prepared catalyst

In this research, the infrared spectroscopy (IR), field emission scanning electron microscopy (FESEM), transmission electron microscopy (TEM), and energy-dispersive X-ray spectroscopy (EDX) techniques were used for characterization of the as-synthesized catalyst.

Infrared (IR)

To identify the presence of various functional groups in the as-prepared catalyst, the IR spectroscopy was used. Figure 2 shows the IR spectra of nano-Fe_3O_4, eggshell, nano-Fe_3O_4@eggshell, and nano-Fe_3O_4@$Ca(HSO_4)_2$ from top to down, respectively. The IR spectrum of Fe_3O_4@eggshell inherits some functional groups as present in the IR spectra of Fe_3O_4 and eggshell. The wave number of 1152 cm^{-1} is related to S=O in the $–SO_3H$ group. In addition, wave numbers from 3000 to 3600 cm^{-1} confirm the OH of the $–SO_3H$ group. These results imply the conversion of $CaCO_3$ to $Ca(HSO_4)_2$ in the synthesis of nano-magnetic catalyst. The functional groups shown by a vertical dash-dotted rectangles (868, 1411, and 2522 cm^{-1}) are present in the eggshell, nano-Fe_3O_4@eggshell, and nano-Fe_3O_4@

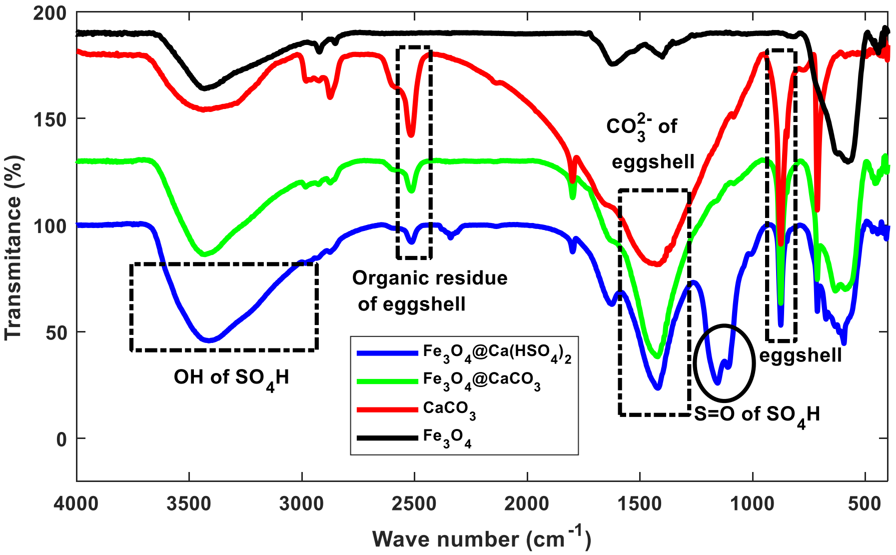

Fig. 2 IR spectra of Fe_3O_4, eggshell, Fe_3O_4@eggshell, and $Fe_3O_4@Ca(HSO_4)_2$

$Ca(HSO_4)_2$. This can be attributed to incomplete conversion of $CaCO_3$ in the presence of chlorosulfonic acid [37]. The generated $Ca(HSO_4)_2$ is solid so that the $ClSO_3H$ has to diffuse through solid $Ca(HSO_4)_2$ to complete the reaction. Accordingly, the reaction between $ClSO_3H$ and $CaCO_3$ is controlled through diffusion which in turn leads to an incomplete reaction.

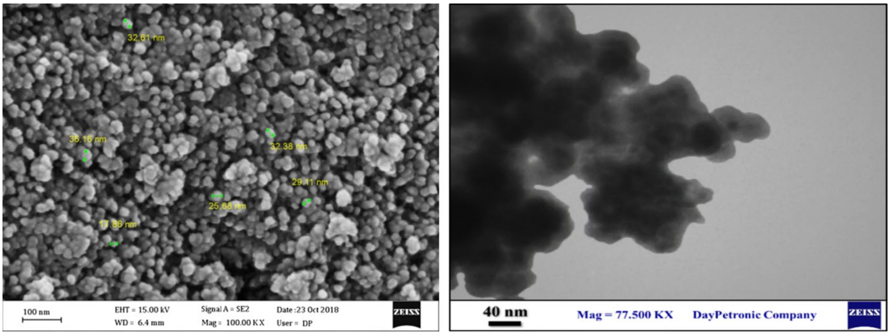

Fig. 3 Field emission scanning electron microscopy (FESEM) and transmission electron microscopy (TEM) of the as-synthesized nano-$Fe_3O_4@Ca(HSO_4)_2$ MNPs

Field emission scanning electron microscopy (FESEM) and transmission electron microscopy (TEM)

The FESEM and TEM are useful techniques in size, shape, and morphology characterization of nanoparticles. TEM provides so useful information, in particular, about the structure of the hybrid materials. Figure 3 illustrates the FESEM (left) and TEM (right) images of the as-synthesized nano-$Fe_3O_4@Ca(HSO_4)_2$. FESEM represents a spherical shape, while TEM shows a core–shell structure for the nanoparticles. Nano-Fe_3O_4, and $Ca(HSO_4)_2$ form the core and shell part of the nanoparticles, respectively. The aggregation of nanoparticles in TEM image can be attributed to the hydrogen bond formation between HSO_4 groups on the nanoparticles surface. The TEM image provides evidence for the formation of the as-synthesized catalyst with a core–shell structure.

Energy-dispersive X-ray spectroscopy (EDX)

The EDX technique provides some information about chemical elements and their relative composition. The accuracy of the obtained results can be affected by some various factors such as the chemical nature of the sample. Figure 4 shows the EDX spectrum of the as-prepared catalyst. The O, C, Fe, S, and Ca are the major constituent atoms, providing consistent evidence for the synthesis procedure. To measure the surface density of HSO_4 groups, back-titration technique was used. 30 mL water, first, was added to a 0.1 g of the as-synthesized catalyst, and the resultant mixture was stirred for 1 h. 10 mL NaOH, then, was added to the mixture and stirred up to the point at which the solution pH was fixed. The solid catalyst, then, was separated from the mixture using an external magnet. Two drops of chemical indicator, finally, (phenolphthalein) was added into the mixture, and the solution was titrated

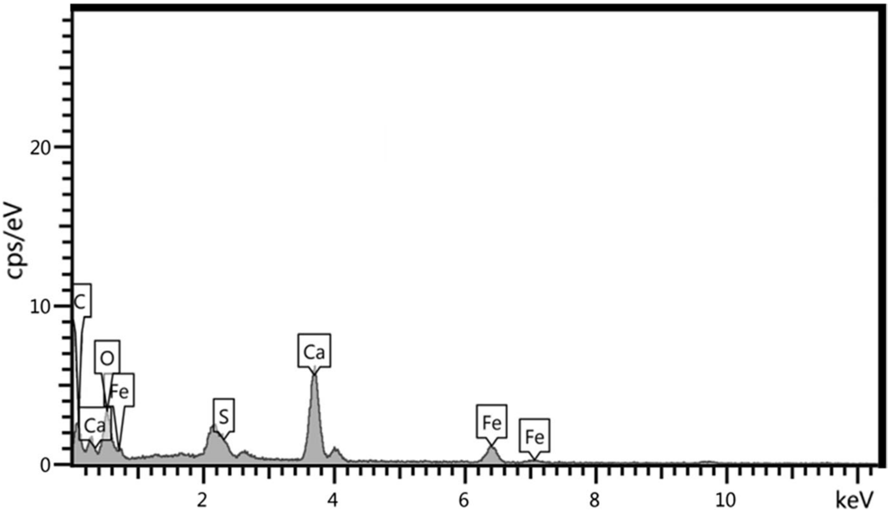

Fig. 4 The energy-dispersive X-ray spectroscopy (EDX) of $Fe_3O_4@Ca(HSO_4)_2$ MNPs

Table 1 Effect of various solvents on the time and yield of reaction 1 (in the presence of a catalyst)

Entry	Solvent	Time (min)	Yield[a] (%) 60 °C
1	–	5	85
2	EtOAc		Trace
3	CH_3CN		Trace
4	H_2O		–
5	*n*-Hexane		Trace
6	EtOH		Trace

[a]Isolated yield

Table 2 Effect of various solvents on time and yield of reaction 2 (in the presence of a catalyst)

Entry	Solvent	Time (min)	Yield[a] (%) 60 °C
1	–	5	94.64
2	EtOAc	10	49.23
3	CH_3CN	10	46.23
4	H_2O	60	–
5	*n*-Hexane	7	68.6
6	EtOH	5	77.84

[a]Isolated yield

against 1.2 mL HCl 0.1 N. Hence, the surface density of acidic groups identified as 8.8 mmol/g catalyst $((10\times0.1-1.2\times0.1)/0.1)$. This quantity shows a large surface density toward the many cases of SO_3H-based reported catalyst in the literature [34]. The more acidic group leads to a more active catalyst in favor of organic transformations.

Evaluation of the catalytic activity of nano-Fe_3O_4@$Ca(HSO_4)_2$

Effect of solvent on the reaction

In order to investigate the effect of solvents on the reaction yield, two benchmark reactions were considered. The reaction among benzaldehyde, acetophenone, ammonium acetate, and malononitrile (reaction 1) and also the reaction among benzaldehyde, ethyl acetoacetate, dimedone, and ammonium acetate (reaction 2) were selected as representative reactions. The Fe_3O_4@$Ca(HSO_4)_2$ was used as the nano-catalyst, and the reactions were carried out in various solvents, including ethanol, ethyl acetate, acetonitrile, water, and n-hexane. The results of the investigated experiments are listed in Tables 1 and 2 for reaction 1 and reaction 2, respectively. Generally, the usage of solvents leads to the low reaction yield. For each benchmark reaction, six cases were tested: reaction at the solvent-free condition, and in the presence of ethyl acetate, acetonitrile, water, n-hexane, and ethanol as solvent. The as-prepared catalyst was used in all six experiments. The solvent-free condition provides the lowest time and highest reaction yield for both benchmark reaction 1 and benchmark reaction 2. For the first benchmark reaction, we find no product in the presence of all six tested solvents. It should be emphasized that benzaldehyde has a dual role, including solvent and reactant in the benchmark reaction 1 and benchmark reaction 2. In the matter of this, the solvent-free condition was chosen for further analysis of the reactions.

Optimization of the reaction condition

Although the optimization of the reaction condition can be done using one-factor-at-a-time method, this method is not efficient, and the cross-effect of factors is not seen. Hence, the central composite design (CCD), in the present work, as a response surface method was used to optimize the both benchmark reaction conditions. Based on the numerical optimization techniques, the optimal condition for benchmark reaction 1 was achieved at 90 °C and 0.05 mol percent of the catalyst. The best value of the temperature and the amount of the catalyst are 71 °C and 0.05 mol percent, respectively, for the benchmark reaction 2. Figure 5 provides the 2D and 3D graphs of the benchmark reaction 1 (a and b) and benchmark reaction 2 (c and d) for yield versus temperature and the amount of the catalyst, respectively. In both reactions, the yield has a direct relation with the amount of catalyst, while there is an optimum

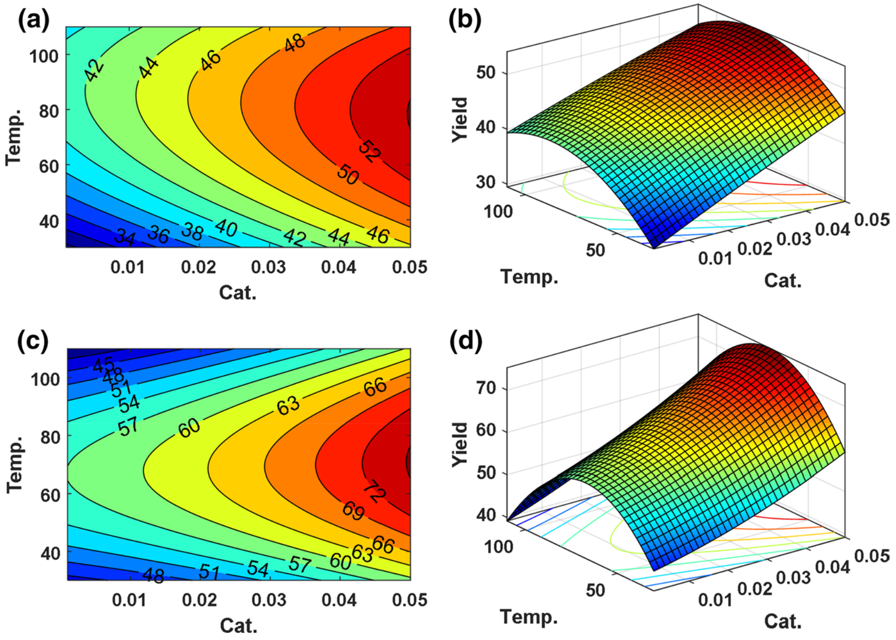

Fig. 5 **a** 2D and **b** 3D graphs for yield versus temperature and the amount of the catalyst. (a and b for benchmark reaction 1; c and d for benchmark reaction 2)

point for the yield versus temperature. The obtained optimum reaction conditions were used to synthesize the different derivatives.

It is assumed that the optimum reaction condition to be the same for all the 2-amino-3-cyanopyridines derivatives. Accordingly, different benzaldehydes with acetophenone, ammonium acetate, and malononitrile were reacted in the presence of the as-prepared catalyst at the optimum condition (0.05 and 90 °C). The reaction times and yields were between 5 and 15 min, and 53–89, respectively (Table 3).

Table 3 Synthesized different 2-amino-4,6-diphenylnicotinonitrile derivatives at the optimum benchmark reaction condition

product	1	2	3	4	5
	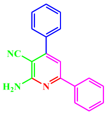	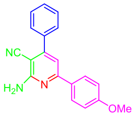	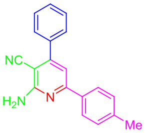	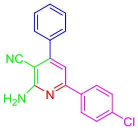	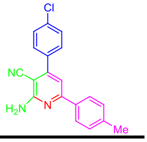
m.p.	182-184	180-187	183-187	246-251	188-191
Yield	85	89.4	66.68	65.58	71.75
Time	5	10	8	10	8
product	6	7	8	9	10
	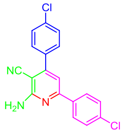	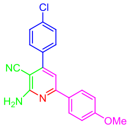	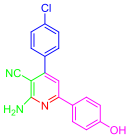	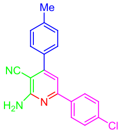	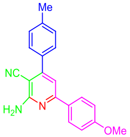
m.p.	198-200	195-197	138	241-243	135-138
Yield	79.34	77.65	62	75.80	65
Time	10	10	10	10	8
product	11	12	13	14	15
	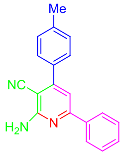	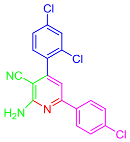	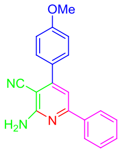	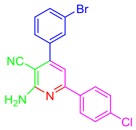	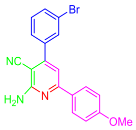
m.p.	137-139	166-168	128	232-237	189-191
Yield	75	63	67.69	67.71	89.07
Time	5	10	13	10	5
product	16	17	18	19	20
	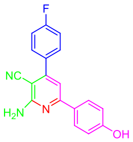	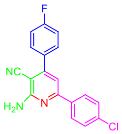	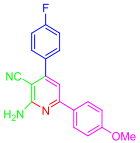	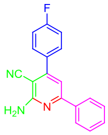	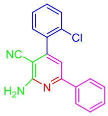
m.p.	247-262	242-243	192-194	161-163	190-191
Yield	63.54	89.07	53	63.04	78.85
Time	5	15	8	10	13
product	21	22			
	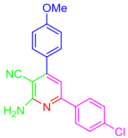	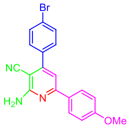			
m.p.	202-203	193-194			
Yield	85.18	85.14			
Time	13	10			

Table 4 Synthesized different hexahydroquinoline derivatives at the optimum benchmark reaction condition

product	1	2	3	4	5
	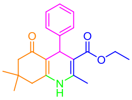	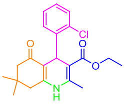	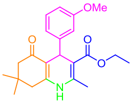	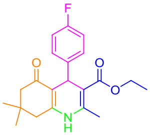	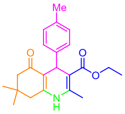
m.p.	218-220	205-207	205-206	186-189 [40]	260-266
Yield	94.64	84.54	87.63	75	86.88
Time	3	5	5	5	5
product	6	7	8	9	10
	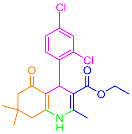	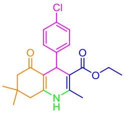	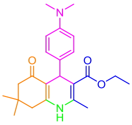	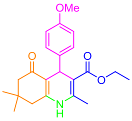	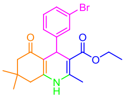
m.p.	242-244 [41]	240-243 [40]	234-236 [42]	257-260	206-208
Yield	91.54	85.4	95	91.52	96.5
Time	7	7	9	5	7
product	11	12			
	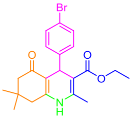	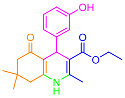			
m.p.	257-262	231-234			
Yield	98.4	67.97			
Time	7	9			

These results imply that the as-prepared catalyst involved in the control step of the reaction which in turn leads to the reduction of activation energy and the reaction time. Yield, time, melting point, and the structures of synthesized derivatives are illustrated in Table 3. In a similar manner, the hexahydroquinoline derivatives were synthesized at the optimal reaction condition (0.05 and 71 °C). Results are listed in Table 4, with the reaction times and yields between 3 and 9 min, and 68–98%, respectively. Table 4 illustrates the yield, time, melting point together with the structure of hexahydroquinoline derivatives. Results confirm the efficiency and involvement of the as-prepared catalyst in the slowest step of the reaction. Reducing organic transformation times leads to an increase in the number of recipe cycles in the industrial production. Conversion of waste to wealth (preparation of the catalyst) and utilizing it in the synthesis of 2-amino-3-cyanopyridines and hexahydroquinoline derivatives are the major objective of the present work.

Proposed mechanism

The suggested plausible mechanism for the synthesis of 2-amino-3-cyanopyridines is shown in Fig. 6, and the possible mechanism for hexahydroquinoline is shown in Fig. 7. Interaction of oxygen atom electrons in benzaldehyde with HSO_4 groups on the catalyst surface provides an active site to attack the malononitrile, and dimedone to benzaldehyde in benchmark reaction 1, and benchmark reaction 2, respectively.

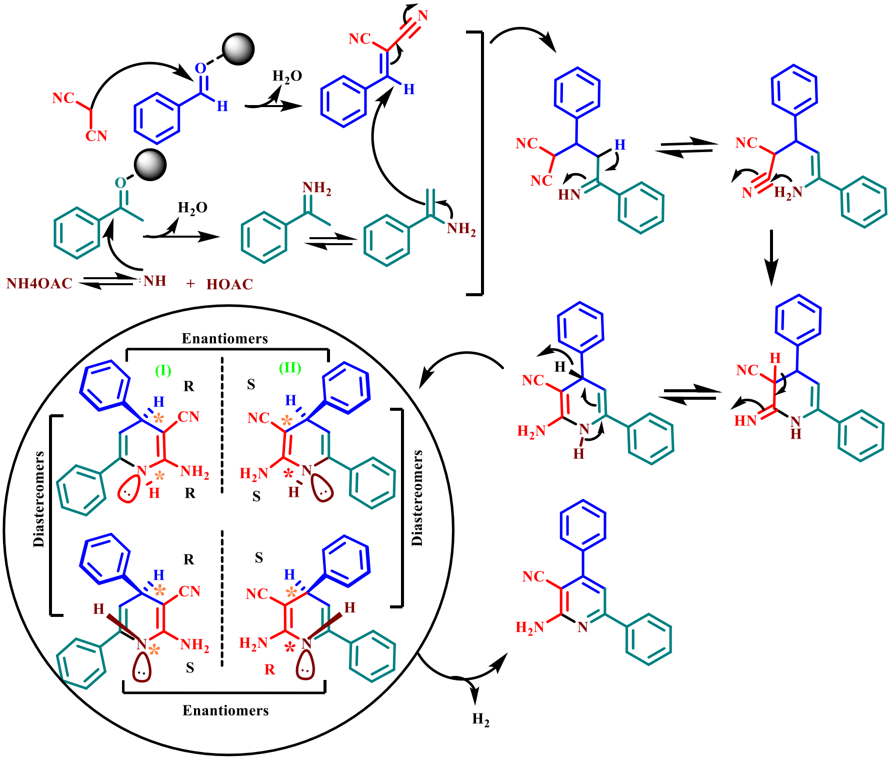

Fig. 6 The proposed mechanism for 2-amino-3-cyanopyridine

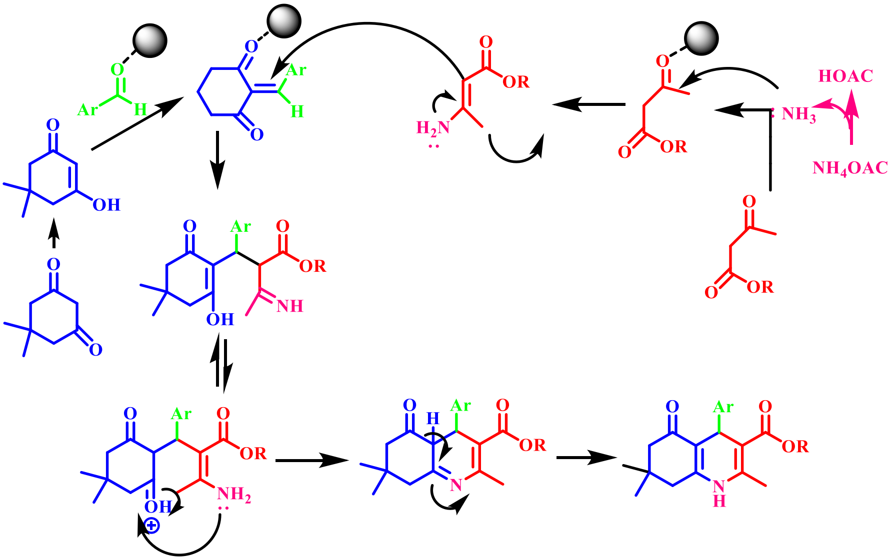

Fig. 7 Possible mechanism for hexahydroquinoline

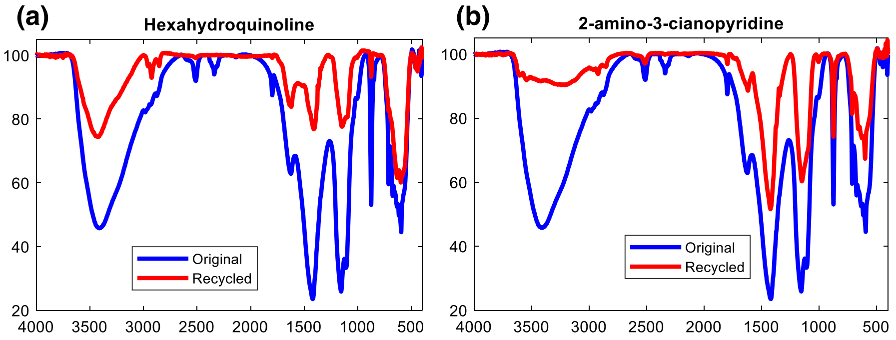

Fig. 8 FT-IR spectra of the original and recycled catalyst in the synthesis of **a** HHQ and **b** 2-A-3-CP

This plausible interaction triggered the multicomponent reaction which, in turn, leads to the formation of products. It should be emphasized that the production of 2-amino-3-cyanopyridines derivatives take places through anomeric-based oxidation (ABO) mechanism [38]. Intermediates I and II have diastereomers which are shown in Fig. 6. It has been shown that the R (I) isomer has a higher oxidation rate than S (II) isomer. In the ABO mechanism, in the other hand, H_2 is generated which is attributed to the hydride transfer owing to the internal molecular orbital (MO) electron transfer in agreement with Marcus theory [39–41].

Retrieval of the catalyst

An efficient catalyst has to perform its role several times without reduction in its activity. Accordingly, the as-prepared catalyst performance was examined in the present work. After the completion of the benchmark reactions, added to the mixture was 20 mL of hot ethanol to dissolve all components except the catalyst. So, the as-prepared catalyst was recovered using an external magnet and dried in an oven after washing several times with ethanol. Recovered catalyst was used in three cycles, and the reaction yield was recorded for both benchmark reactions (94, 93, and 91% for the benchmark reaction 1 and 85, 87, and 79% for the benchmark reaction 2). This result confirms the stability of the as-prepared catalyst in different cycles. The FT-IR technique, also, was used to investigate the stability of the catalyst in each cycle. The identical FT-IR spectra (Fig. 8a and b) in all cycles confirm the chemical stability of the as-prepared catalyst.

Conclusion

The current study found a route to the conversion of eggshell waste to a valuable solid catalyst. Different metrics confirmed the stability and efficiency of the as-prepared solid acid catalyst in the organic transformations. The as-prepared catalyst, strictly speaking, has a high potential to be used in organic synthesis. The optimum reaction condition, as the present work, should be identified via the design of experiment. Using the as-prepared catalyst, the reaction time can be considerably reduced. High yield, short reaction time, solvent-free condition, wastes to wealth conversion, and optimization with the design of expert are the major advantages of the present work. Hope this work motivates the researcher to prepare catalyst from the available waste in the world. So, further investigation and experimentation into waste to wealth conversion is strongly recommended.

Acknowledgements The authors gratefully acknowledge the Bu-Ali Sina University Research Council and Center of Excellence in Development of Environmentally Friendly Methods for Chemical Synthesis (CEDEFMCS) for providing support for this work.

References

1. Z. Chen, Q. Zhu, W. Su, Tetrahedron Lett. **52**, 20 (2011)
2. J.-P. Wan, S.-F. Gan, G.-L. Sun, Y.-J. Pan, J. Org. Chem. **74**, 7 (2009)
3. S. Gao, C.H. Tsai, C. Tseng, C.-F. Yao, Tetrahedron **64**, 38 (2008)
4. T.-S. Jin, Y. Yin, L.-B. Liu, T.-S. Li, Arkivoc **14** (2006)
5. S. Kumar, P. Sharma, K.K. Kapoor, M.S. Hundal, Tetrahedron **64**, 3 (2008)
6. A. Mulik, D. Chandam, P. Patil, D. Patil, S. Jagdale, M. Deshmukh, J. Mol. Liq. **179** (2013)
7. A. Jashari, E. Hey-Hawkins, B. Mikhova, G. Draeger, E. Popovski, Molecules **12**, 8 (2007)
8. É. Lukevits, Chem. Heterocycl. Compd. **31**, 6 (1995)
9. R. Ghorbani-Vaghei, Z. Toghraei-Semiromi, R. Karimi-Nami, C. R. Chim. **16**, 12 (2013)
10. S. Kambe, K. Saito, A. Sakurai, H. Midorikawa, Synthesis **1980**, 05 (1980)
11. S. Chen, C. Qin, J.E. Sin, X. Yang, L. Tao, X. Zeng, P. Zhang, C.M. Gao, Y.Y. Jiang, C. Zhang, Y.Z. Chen, W.K. Chui, Future Med. Chem. **9**, 1 (2016)
12. J. Deng, T. Sanchez, L.Q. Al-Mawsawi, R. Dayam, R.A. Yunes, A. Garofalo, M.B. Bolger, N. Neamati Bioorg, Med. Chem. **15**, 14 (2007)
13. T. Murata, M. Shimada, S. Sakakibara, T. Yoshino, H. Kadono, T. Masuda, M. Shimazaki, T. Shintani, K. Fuchikami, K. Sakai, H. Inbe, K. Takeshita, T. Niki, M. Umeda, K.B. Bacon, K.B. Ziegelbauer, T.B. Lowinger Bioorg. Med. Chem.Lett. **13**, 5 (2003)
14. M. Mantri, O. de Graaf, J. van Veldhoven, A. Göblyös, J.K. von Frijtag Drabbe Künzel, T. Mulder-Krieger, R. Link, H. de Vries, M.W. Beukers, J. Brussee, A.P. Ijzerman, J. Med. Chem. **51**, 15 (2008)
15. M.A. Gouda, M.A. Berghot, G.E. Abd El Ghani, A.E.-G.M. Khalil, Synth. Commun. **44**, 3 (2014)
16. A.A. Dissanayake, R.J. Staples, A.L. Odom, Adv. Synth. Catal. **356**, 8 (2014)
17. J. Tang, L. Wang, Y. Yao, L. Zhang, W. Wang, Tetrahedron Lett. **52**, 4 (2011)
18. M.M. Heravi, S. Yahya Shirazi Beheshtiha, M. Dehghani, N. Hosseintash, J. Iran. Chem. Soc. **12**, 11 (2015)
19. J.-F. Zhou, Y.-Z. Song, J.-S. Lv, G.-X. Gong, S. Tu, Synth. Commun. **39**, 8 (2009)
20. T. Shintani, H. Kadono, T. Kikuchi, T. Schubert, Y. Shogase, M. Shimazaki Tetrahedron Lett. **44**, 35 (2003)
21. S. Khaksar, M. Yaghoobi, J. Fluor. Chem. **142** (2012)
22. L. Srinivasula Reddy, T. Ram Reddy, N.C. Gangi Reddy, R.B. Mohan, Y. Lingappa, J. Heterocycl. Chem. **51**, S1 (2014)
23. A.L. Odom, T.J. McDaniel, Acc. Chem. Res. **48**, 11 (2015)
24. R. Khalifeh, M. Ghamari, J. Braz. Chem. Soc. **27** (2016)
25. R. Gupta, A. Jain, M. Jain, R. Joshi, Bull. Korean Chem. Soc. **31**, 11 (2010)
26. M.A. Zolfigol, M. Kiafar, M. Yarie, A. Taherpour, M. Saeidi-Rad, RSC Adv. **6**, 55 (2016)
27. S.S. Mansoor, K. Aswin, K. Logaiya, P.N. Sudhan, S. Malik, Res. Chem. Intermediat. **40**, 2 (2014)
28. M. Abdollahi-Alibeik, N. Sadeghi-Vasafi, A. Moaddeli, A. Rezaeipoor-Anari, Res. Chem. Intermediat. **42**, 4 (2016)
29. D. Khalili, Tetrahedron Lett. **57**, 15 (2016)
30. F. Tamaddon, S. Ghazi, M.R. Noorbala, J. Mol. Catal. B Enzym., **127** (2016)
31. J. Tong-Shou, W. Ai-Qing, S. Feng, H. Li-Sha, L. Li-Bin, L. Tong-Shuang, Arkivoc, **14** (2006)

32. Z. Han, J. Lv, J. Zhang, Tetrahedron **75**, 14 (2019)
33. S. Talaiefar, S.M. Habibi-Khorassani, M. Sharaki, E. Mollashahi, Polycycl. Aromat. Comp. (2019). https://doi.org/10.1080/10406638.2019.1570953
34. A. Khazaei, N. Sarmasti, J.Y. Seyf, App. Organomet. Chem. **32**, 4 (2018)
35. X. Liu, Z. Ma, J. Xing, H. Liu, J. Magn. Magn. Mater. **270**, 1–2 (2004)
36. R. Taylor, H.A. Kooijman. Chem. Eng. Commun. **102**, 1 (1991)
37. R.B. Bird, W.E. Stewart, E.N. Lightfoot, Transp. Phenom. (Wiley, 2007)
38. M. A. Zolfigol, M. Kiafar, M. Yarie, A. Taherpour, M. S. Rad, RSC Adv. **6**, 50100 (2016)
39. R. A. Marcus, Rev. Mod. Phys. **65**, 599 (1993)
40. M. Andrea, MPIP J. Club Mainz. **29** (2008)
41. S. Salehzadeh, RSC Adv. **7**, 39704 (2017)